EPJ manuscript No.
(will be inserted by the editor)

Direct Photons, Vector Mesons and Heavy Flavor Production at RHIC

K.F. Read[1,2]

[1] Physics Division, Oak Ridge National Laboratory, Oak Ridge, TN 37831, USA, e-mail: readkf@ornl.gov
[2] Department of Physics and Astronomy, University of Tennessee, Knoxville, TN 37996, USA

Received: date / Revised version: date

Abstract. Recent results concerning the production of direct photons, vector mesons, charmonium, and open heavy flavor in $p+p$, $d+Au$, and $Au+Au$ collisions at $\sqrt{s_{NN}} = 200$ GeV at RHIC are discussed. The production of direct photons in $Au+Au$ collisions does not exhibit a centrality-dependent suppression at higher transverse momentum such as that observed for hadrons at RHIC. Rather, it is well-described by predictions based on NLO pQCD scaled by the number of binary nucleon-nucleon collisions. Measurements of ϕ production do exhibit a suppression in central $Au+Au$ collisions relative to scaled peripheral collisions and scaled $p+p$ collisions consistent with expectations of recombination models. Measurements of J/ψ production using dielectrons and dimuons exhibit a suppression rather than an enhancement in central $Au+Au$ collisions as predicted by some recent models. Open heavy flavor production has been measured via semileptonic decays of heavy quarks as well as direct reconstruction of charmed mesons. In $Au+Au$ collisions, although the total yield does scale by the number of binary collisions, the spectrum exhibits a strong modification relative to scaled results based on $p+p$ collisions. Measurements of the azimuthal anisotropy parameter v_2 for electrons resulting from charm meson decay in $Au+Au$ collisions are consistent with calculations in which charm quarks participate in the collective flow of the produced medium.

1 Introduction

A wealth of exciting data has been collected by the four RHIC experiments: BRAHMS [1], PHENIX [2], PHOBOS [3], and STAR [4]. Analysis of $p+p$, $d+Au$, $Cu+Cu$, and $Au+Au$ collisions at $\sqrt{s_{NN}} = 200$ GeV has yielded a broad range of important new results. In this paper we confine our attention to recent results concerning direct photons, vector mesons, and heavy flavor production.

Direct photons are an important probe in heavy ion nuclear collisions since they are relatively unaffected by the strongly interacting produced matter. Measurements of the production of direct photons can be used to discriminate whether initial or final state effects are responsible for the centrality-dependent suppression of hadron production at higher transverse momentum observed at RHIC [1–4].

The transverse momentum distribution of the nuclear modification ratio R_{CP} (defined below) of the ϕ meson production cross section in central $Au+Au$ collisions to that of scaled peripheral collisions can be used to test partonic recombination scenarios and further study the issue of hadron suppression at RHIC.

Measurements of open heavy flavor and charmonium production in $p+p$ collisions can be used to test pQCD predictions at $\sqrt{s} = 200$ GeV as well as establish a baseline for interpreting charm production in heavy ion collisions. The results of such measurements for $d+Au$ collisions are used to test predictions for modification of the gluon structure function in nuclei (shadowing). Such measurements for $Au+Au$ collisions at $\sqrt{s_{NN}} = 200$ GeV can be used to study medium modification effects such as charm quark energy loss and collective flow. They can be used to search for evidence of thermal production of charm from a possible Quark Gluon Plasma and to study predicted modifications to J/ψ production due to the produced medium.

Nucleus-nucleus collisions are classified according to *centrality*, defined to be the percentile of the total geometrical cross section (with 0% − 5% representing the most central collisions), a quantity which is related to impact parameter. At RHIC, the centrality measurement for a collision is based on a correlation of the measured charge sum in beam-beam counters (BBC) and total forward energy deposited in zero-degree calorimeters (ZDC) [5] using a Glauber Monte Carlo [6] incorporating the BBC and ZDC response. Using this model, the average number of binary nucleon-nucleon inelastic collisions, N_{coll}, can be computed for a given centrality [5]. Many of the (rare) processes investigated at RHIC and discussed below result from point-like hard scattering involving small cross sections. To the extent that $Au+Au$ collisions behave as an incoherent superposition of $p+p$ collisions, the ratio of the cross section for such hard processes in $Au+Au$ collisions compared to $p+p$ collisions at the same value of $\sqrt{s_{NN}}$ is expected to be proportional to N_{coll} for the given centrality class [2].

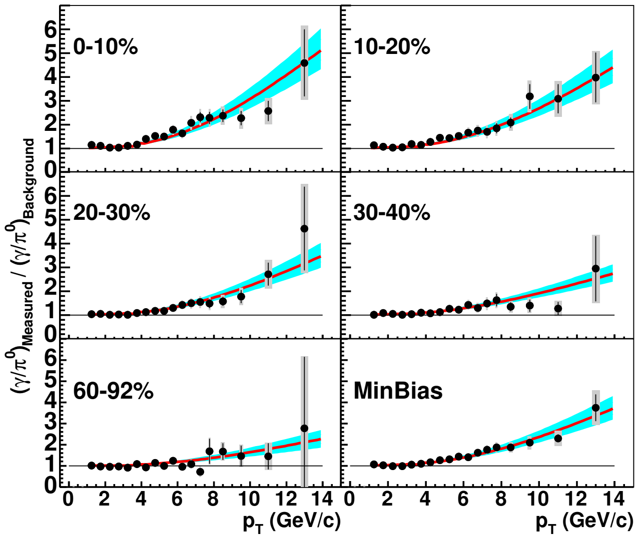

Fig. 1. Transverse momentum distribution of the ratio of the corrected inclusive photon yield compared to the background decay photon yield for different centrality bins for minimum bias $Au + Au$ collisions at $\sqrt{s_{NN}} = 200$ GeV [7]. The curves correspond to unity plus the ratio of an NLO pQCD prediction, scaled by N_{coll}, to the decay photon yield for each centrality bin.

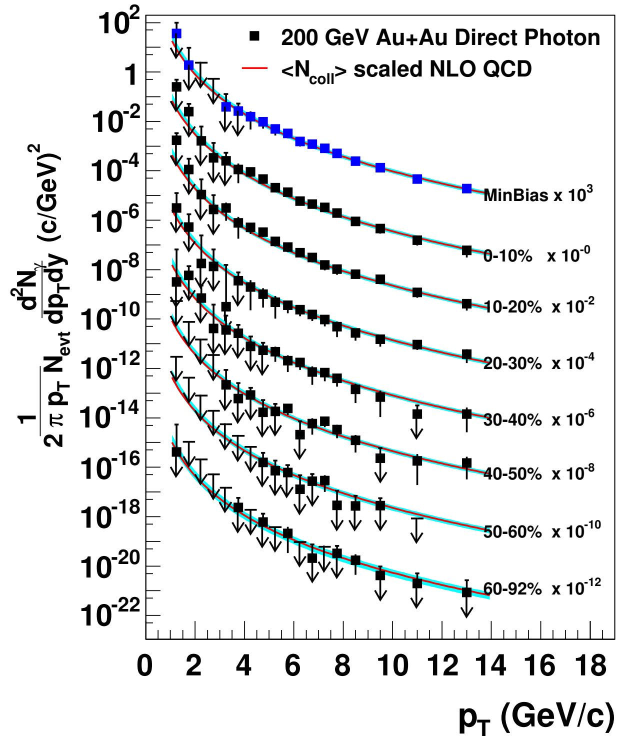

Fig. 2. Transverse momentum distribution of the invariant yield of direct photons for $Au + Au$ collisions at $\sqrt{s_{NN}} = 200$ GeV for different centrality bins, scaled by successive powers of 10 for clarity [7]. The curves indicate the corresponding scaled NLO pQCD predictions.

2 Direct Photons

The following double ratio

$$\frac{\gamma^{Inclusive}/\pi^0}{\gamma^{Decay}/\pi^0} \approx \frac{\gamma^{Decay} + \gamma^{Direct}}{\gamma^{Decay}} \tag{1}$$

for minimum bias $Au+Au$ collisions at $\sqrt{s_{NN}} = 200$ GeV is displayed in Figure 1. An excess of direct photons is observed at higher transverse momentum that increases with centrality [7]. The results are consistent with NLO pQCD predictions scaled by N_{coll}.

The invariant yield of direct photons in $Au + Au$ collisions at $\sqrt{s_{NN}} = 200$ GeV is shown in Figure 2. The curves indicate the scaled NLO pQCD predictions for each centrality class. Within errors, the scaled predictions describe the photon yield well.

The centrality dependence of the nuclear modification ratio

$$R_{AA}(p_T, y; b) = \frac{d^2N_{AA}/dydp_T}{\langle T_{AA}(b)\rangle d^2\sigma_{pp}/dydp_T} \tag{2}$$

for transverse momenta above 6.0 GeV/c is displayed in Figure 3 [7]. For this figure, N_{part}, the average number of nucleons participating in the collision based on a Glauber Model calculation for a given centrality class, is used as a measure of centrality. The transverse momentum distribution of the nuclear modification factors for direct photons (squares) and hadrons in central $Au + Au$ collisions are displayed in Figure 4. Direct photons do not exhibit the suppression at higher transverse momentum observed for hadrons [8]. This important result provides strong evidence that the hadron suppression is due to a final state effect (such as parton energy loss).

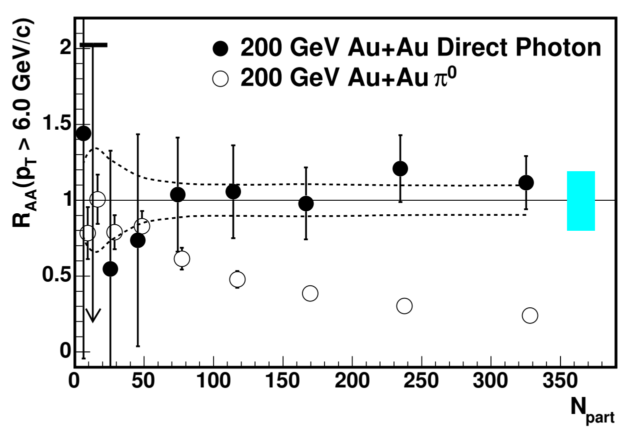

Fig. 3. Nuclear modification factor R_{AA} (defined in text) for direct photon (solid circles) and π^0 (open circles) production in $Au + Au$ collisions at $\sqrt{s_{NN}} = 200$ GeV versus the calculated number of participants for transverse momenta above 6.0 GeV/c [7].

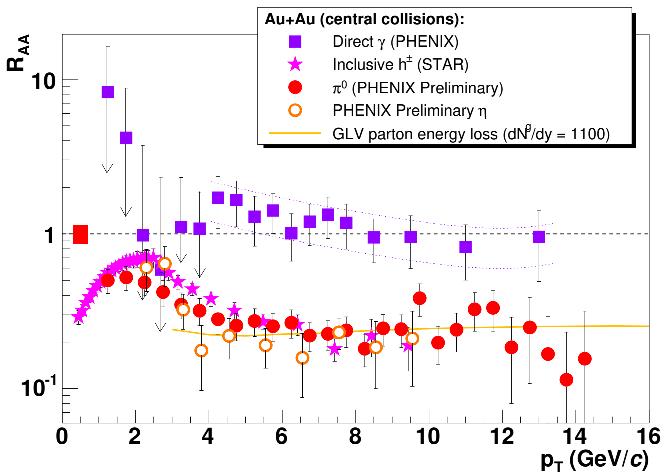

Fig. 4. Transverse momentum distribution of the nuclear modification factor R_{AA} (defined in text) for direct photon (squares) and π^0 (solid circles) production in central $Au + Au$ collisions at $\sqrt{s_{NN}} = 200$ GeV [8].

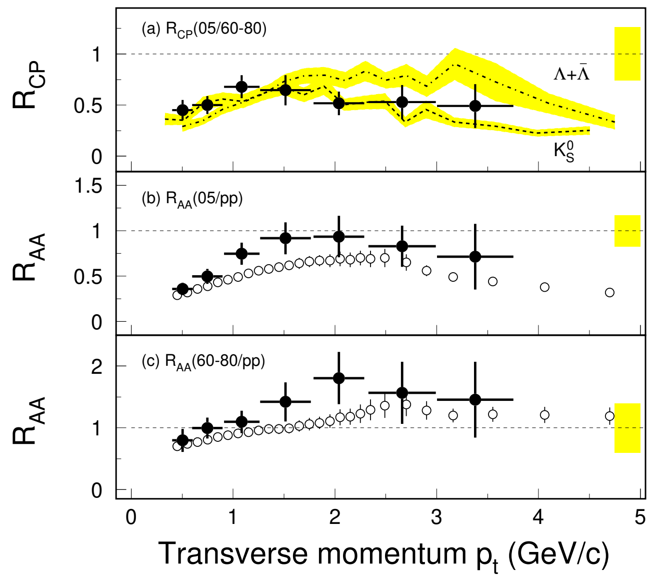

Fig. 5. STAR transverse momentum distribution of the nuclear modification ratio of the ϕ meson production cross section (solid circles) for (a) central $Au + Au$ relative to scaled peripheral $Au + Au$ results, (b) central $Au + Au$ relative to scaled $p + p$ results, and (c) peripheral $Au + Au$ relative to scaled $p + p$ results at $\sqrt{s_{NN}} = 200$ GeV [9]. The corresponding nuclear modification factors R_{AA} for charged hadrons (open circles) are shown in panels (b) and (c) for comparison.

The suppression of high transverse momentum π^0's in central $Au + Au$ collisions at RHIC greatly increases the ratio $\gamma^{Direct}/\gamma^{Decay}$, making direct photons much easier to measure. Future measurements with reduced errors will enable searches for deviations from pQCD and evidence for other contributions, e.g. thermal photons.

3 Vector Mesons

Vector meson production is a broad area of investigation at RHIC. In this section we confine the discussion to aspects of ϕ meson production.

The ratio of the ϕ meson invariant yield for central compared to peripheral $Au + Au$ collisions scaled by the relative values of N_{coll} is displayed in Figure 5a [9] and referred to as the nuclear modification factor R_{CP}. The production of ϕ mesons is suppressed in central $Au + Au$ collisions. The ratio R_{CP} for ϕ mesons is comparable to that for pions rather than protons, a pattern which is consistent with partonic recombination scenarios [9,10].

Measurement of the ϕ meson invariant yield can be used to further test models for hadron suppression at RHIC and to study the anomalous proton to pion ratio observed in central $Au + Au$ collisions at RHIC [10].

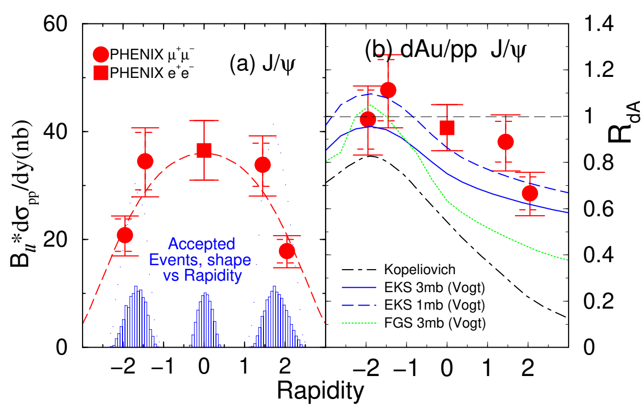

Fig. 6. (a) Rapidity distribution of branching ratio times differential J/ψ production cross section for dimuons (circles) and dielectrons (squares) for $p + p$ collisions at $\sqrt{s} = 200$ GeV. (b) Rapidity distribution of the nuclear modification ratio of the J/ψ production cross section for $d + Au$ collisions compared to $p + p$ collisions scaled by N_{coll} at $\sqrt{s_{NN}} = 200$ GeV [11].

4 Heavy Flavor Production

The J/ψ differential production cross section has been measured in $p + p$, $d + Au$, $Cu + Cu$, and $Au + Au$ collisions at RHIC. The J/ψ differential production cross section for $p + p$ collisions at $\sqrt{s} = 200$ GeV is shown in Figure 6a [11]. The measurement yields a total cross section of $\sigma_{pp}^{J/\psi} = 2.61 \pm 0.20\,(\mathrm{fit}) \pm 0.26\,(\mathrm{abs})\ \mu$b. A nuclear dependence is observed in the rapidity distribution of J/ψ production in $d + Au$ collisions compared to scaled $p + p$

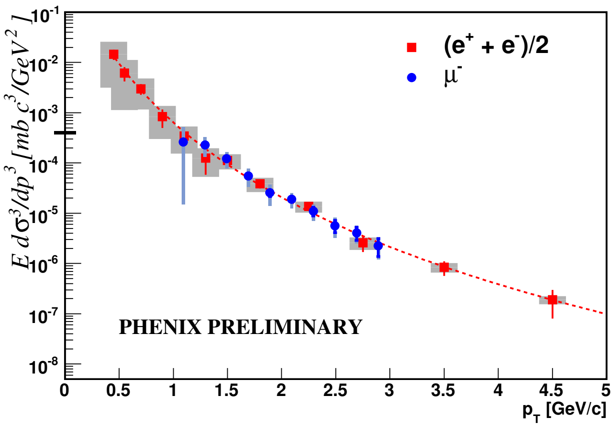

Fig. 7. Preliminary transverse momentum distribution of invariant differential production cross section for negative muons (circles) and the average of electrons and positrons (squares) from heavy flavor decay for $p+p$ collisions at $\sqrt{s} = 200$ GeV. The pseudorapidity interval is centered around $|\eta| = 1.65$ for muons and $\eta = 0$ for electrons and positrons. Systematic errors are indicated as shaded bands. The systematic error associated with the overall normalization of the muon data is separately indicated by the horizontal band on the vertical axis. The dashed curve is a power law fit to the electron data points.

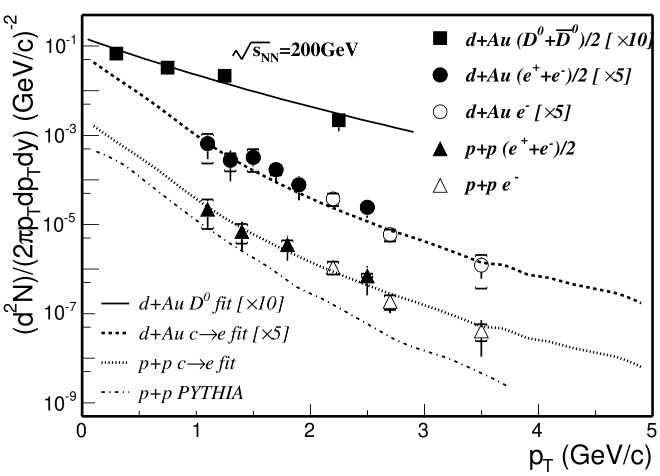

Fig. 8. STAR transverse momentum distribution of reconstructed D^0 mesons (solid squares) for $d+Au$ collisions and non-photonic electrons for $p+p$ (triangles) and $d+Au$ (circles) collisions at $\sqrt{s_{NN}} = 200$ GeV [13].

results (Fig. 6b) [11]. The ratio is near unity at backward rapidity and significantly lower at forward rapidity. Such measurements test predictions concerning modification of the gluon structure function in nuclei.

Measurements of J/ψ production in $Au+Au$ collisions [12] disfavor models with strong enhancement of production. Results based on a susbequent run with increased statistics and different colliding species ($Cu+Cu$) are in preparation.

After subtraction of physics backgrounds, measurement of single electrons and positrons ("non-photonic electrons")

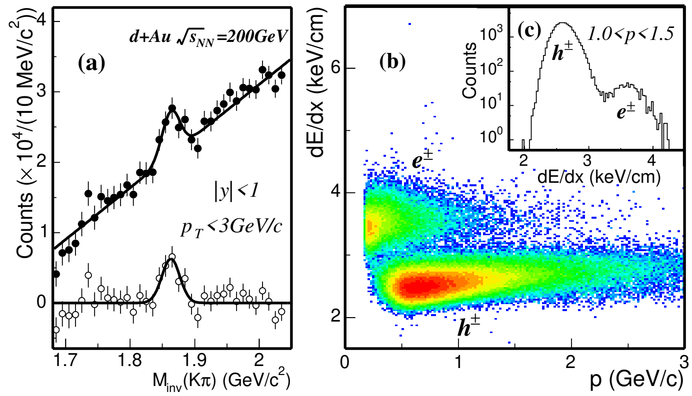

Fig. 9. (a) STAR $K\pi$ invariant mass distribution for $d+Au$ collisions at $\sqrt{s_{NN}} = 200$ GeV after mixed-event background subtraction (solid circles) and subsequent linear residual background subtraction (open circles) [13] ; (b) momentum distribution of dE/dx in the STAR TPC [13].

and single muons can be used to determine the production of heavy quarks. The transverse momentum distribution of the production cross section for muons and non-photonic electrons from heavy flavor decay for $p+p$ collisions is displayed in Figure 7. The pseudorapidity interval is centered around $|\eta| = 1.65$ for muons and $\eta = 0$ for electrons and positrons. The transverse momentum distribution of non-photonic electrons for $p+p$ collisions at $\sqrt{s} = 200$ GeV is also shown in Figure 8 along with the corresponding plot for $d+Au$ collisions at $\sqrt{s_{NN}} = 200$ GeV.

Exclusive reconstruction of charmed mesons (Fig. 9) can be used to measure open charm production more directly. The D^0 meson invariant yield for $d+Au$ collisions at $\sqrt{s_{NN}} = 200$ GeV is shown in Figure 8 [13].

The transverse momentum distribution of non-photonic electrons in $Au+Au$ collisions at $\sqrt{s_{NN}} = 200$ GeV is shown in Figure 10. The data exhibit a suppression at higher transverse momentum relative to scaled $p+p$ results. The spectral shape is modified by the produced medium. The pattern is consistent with models incorporating heavy quark energy loss [14].

The initial state spatial anisotropy of the collision reaction zone leads to a final state momentum anisotropy. This results in asymmetric particle emission. The second component of a Fourier decomposition of the azimuthal distribution of particles, v_2, indicates the degree of azimuthal anisotropy:

$$E\frac{d^3N}{d^3p} = \frac{d^3N}{p_T d\phi dp_T dy} \sum_{n=0}^{n=\infty} 2v_n \cos(n(\phi - \Psi_{R.P.})) \qquad (3)$$

where $\Psi_{R.P.}$ is the direction of the nuclear impact parameter ("reaction plane") in a given collision.

Preliminary PHENIX and STAR measurements of the momentum distribution of the azimuthal anisotropy parameter, v_2, are displayed in Figure 11 [15,16]. The STAR results extend the measurement of this parameter from 1.5 to 3.0 GeV/c.

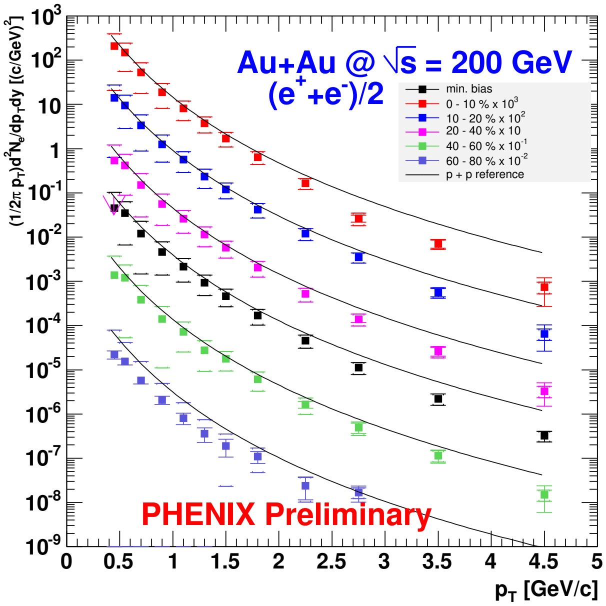

Fig. 10. Preliminary transverse momentum distribution of non-photonic electrons in $Au + Au$ collisions at $\sqrt{s_{NN}} = 200$ GeV for different centrality bins, scaled by successive powers of 10 for clarity. The curves correspond to $p+p$ collision results scaled by N_{coll} for each centrality bin.

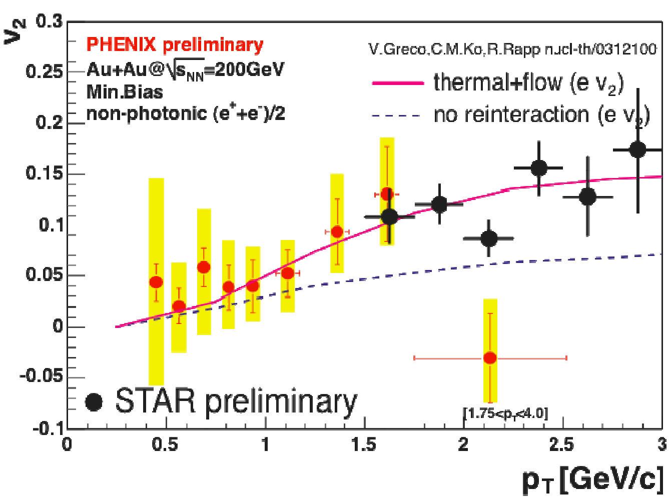

Fig. 11. PHENIX and STAR preliminary transverse momentum distributions of v_2 (defined in text) for non-photonic electrons in minimum bias $Au+Au$ collisions at $\sqrt{s_{NN}} = 200$ GeV [15,16]. The curves indicate two different models concerning charm flow [17].

5 Summary and Conclusions

NLO pQCD predictions provide a good description of direct γ and π^0 production for $p+p$ collisions at $\sqrt{s} = 200$ GeV. Direct γ production in $Au+Au$ collisions at $\sqrt{s_{NN}} = 200$ GeV is consistent with results based on both $p+p$ data and NLO pQCD predictions scaled by N_{coll}. This supports the hypothesis that the observed hadron suppression at higher transverse momentum in central $Au + Au$ collisions is due to a final state effect, such as parton energy loss. The suppression of the production of ϕ mesons in central $Au + Au$ collisions is consistent with partonic recombination scenarios. Heavy flavor production has been measured via semileptonic decays in $p + p$, $d + Au$, and $Au + Au$ collisions at $\sqrt{s_{NN}} = 200$ GeV. Data concerning heavy flavor production in $p+p$ and $d+Au$ collisions serve as an important baseline for interpreting heavy flavor production in $Au + Au$ collisions. Measurements of $\sigma_{c\bar{c}}$ at RHIC provide an important test of pQCD predictions. A strong modification is observed for the spectra of non-photonic electrons in $Au + Au$ collisions compared to results from $p+p$ collisions scaled by N_{coll}. Measurements of the azimuthal anisotropy parameter v_2 of non-photonic electrons in $Au + Au$ collisions are consistent with models incorporating elliptic flow of the charm quark [17].

Acknowledgements. This research was sponsored by the Division of Nuclear Physics, U.S. Department of Energy, under contract DE-AC05-00OR22725 with UT-Battelle, LLC (Oak Ridge National Laboratory) and contract DE-FG02-96ER40982 with the University of Tennessee. T. Ullrich provided information concerning recent results from the STAR Collaboration.

References

1. BRAHMS Coll., I. Arsene, et al., Nucl. Phys. A **757**, 1 (2005)
2. PHENIX Coll., K. Adcox, et al., Nucl. Phys. A **757**, 184 (2005)
3. PHOBOS Coll., B.B. Back, et al., Nucl. Phys. A **757**, 28 (2005)
4. STAR Coll., J. Adams, et al., Nucl. Phys. A **757**, 102 (2005)
5. PHENIX Coll., K. Adcox, et al., Phys. Rev. C **69**, 024909 (2004)
6. R. Glauber and J. Natthiae, Nucl. Phys. B **21**, 135 (1970)
7. PHENIX Coll., K. Adcox, et al., Phys. Rev. Lett. **94**, 232301 (2005)
8. D. d'Enterria, Eur. Phys. J. C **43**, 295 (2005)
9. STAR Coll., J. Adams, et al., Phys. Lett. B **612**, 181 (2005)
10. PHENIX Coll., S.S. Adler, et al., Phys. Rev. C **72**, 014903 (2005)
11. PHENIX Coll., S.S. Adler, et al., nucl-ex/0507032 (2005)
12. PHENIX Coll., S.S. Adler, et al., Phys. Rev. C **69**, 014901 (2004)
13. STAR Coll., J. Adams, et al., Phys. Rev. Lett. **94**, 062301 (2005)
14. Y.L. Dokshitzer and D.E. Kharzeev, Phys. Lett. B **519**, 199 (2001)
15. PHENIX Coll., S.S. Adler, et al., Phys. Rev. C **72**, 024901 (2005)
16. STAR Coll., F. Laue, et al., J. Phys. G: Nucl. Part. Phys. **31**, S27 (2005); STAR Coll., F. Laue, et al., J. Phys. G: Nucl. Part. Phys. **31**, S11211 (2005)
17. V. Greco, C.M. Ko, R. Rapp, Phys. Lett. B **595**, 202 (2004); V. Greco, C.M. Ko, R. Rapp, nucl-th/0312100 (2004)